Computational principles of neural adaptation for binaural signal integration

Timo Oess[*,1,2], Marc O. Ernst[1], Heiko Neumann[2]

1 Applied Cognitive Psychology, Ulm University, Ulm, Germany
2 Institute of Neural Information Processing, Ulm University, Ulm, Germany

* timo.oess@uni-ulm.de

Short Title: Neural adaptation in binaural signal integration

Abstract

Adaptation to statistics of sensory inputs is an essential ability of neural systems and extends their effective operational range. Having a broad operational range of sensory inputs facilitates the ability to react to very different sensory inputs, thus is a crucial factor for survival. Adaptation mechanisms are found at many stages of sensory pathways of various modalities.

The computation of auditory cues for localization of sound sources, particularly the interaural level difference (ILD), has long been considered as a static process. Recent findings suggest that this process of ipsi- and contra-lateral signal integration is highly adaptive and depends strongly on experienced stimulus statistics. Here, adaptation aids the encoding of auditory perceptual space of various granularities. To investigate the mechanism of auditory adaptation in binaural signal integration in detail, we developed a neural model architecture of canonical principles for simulating functions of lateral superior olive (LSO) and medial nucleus of the trapezoid body (MNTB) composed of single compartment conductance-based neurons. Neurons in the MNTB serve as an intermediate relay population and their signal is integrated by the LSO population on a circuit level to represent excitatory and inhibitory interactions of input signals. The circuit incorporates a novel adaptation mechanism operating at the synaptic level based on local inhibitory feedback signals. The model's predictive power is demonstrated in various simulations replicating physiological data. Incorporating the novel adaptation mechanism facilitates a shift in neural responses towards the most effective stimulus range based on recent stimulus history. The model demonstrates that a single LSO neuron quickly adapts to recent stimulus statistics and, thus, can encode the entire range of ILDs in the ipsilateral hemisphere. Most significantly, we provide a unique measurement index of the adaptation efficacy of LSO neurons. Prerequisite of normal function is an accurate interaction of inhibitory and excitatory signals, a precise encoding of time and a well-tuned local feedback circuit. We suggest that the mechanisms of temporal competitive-cooperative interaction and the local feedback mechanism jointly sensitize the circuit to enable a response shift towards contra-lateral and ipsi-lateral stimuli, respectively.

Author summary

Why are we better in localizing a sound after hearing it several times? Neural adaptation to stimuli statistics plays a crucial role in this and the present article

investigates the abilities of a neural adaptation mechanism for improved localization skills based on a neural modal. Adaptation to stimuli statistics is very prominent in sensory system of animals and allows them to respond to a wide range of stimuli, thus is a crucial factor for survival. For example, humans are able to recognize objects in very bright environments (driving a car against the direction of sunlight) but also in almost complete darkness (finding the way to the toilet at night). This is possible by courtesy of adaptation abilities of our sensory organs and pathways. Certainly, adaptation is not confined to a single sense like vision but also affects other senses like audition. Especially the perception of sound source location. Here, it allows focusing on a specific part of auditory space and thereby facilitates improved localisation abilities. Localization of a sound source in the horizontal plane is a rather complicated task for animals. It requires the underlying neural system to compute differences of the intensity between the two ears which provide a distinct cue for the location of sound sources. Based on recent findings that suggest that the intensity difference computation is a flexible process with distinct adaptation mechanisms, we developed a neural model that computes the intensity difference to two incoming sound signals. The model comprises a novel mechanism for adaptation to sound source locations and provides a means to investigate underlying neural principles of adaptation and compare their effectivenesses. We demonstrate that due this mechanism the perceptual range is extended and a finer resolution of auditory space is be obtained. Results explain the neural basis for adaptation and indicate that the interplay between different adaptation mechanisms facilitate highly precise sound source localization in a wide range of locations.

Introduction

Localization of a sound source in space is a crucial task for every living being that is facilitated with an auditory system, may it be for hunting or predator avoidance. In contrast to visual object localization which is limited to the front view, auditory localization allows for detection of sound sources in 360°. It works in low contrast environments (bright day light or complete darkness) and some animals solely rely on auditory localization to hunt and find their way through an environment [1, 2]. Humans take advantage of their accurate sound source localization system e.g. to focus on a single speaker among plenty other sources (see *cocktail party effect* [3]).

Auditory localization is a rather complicated task, since a sound signal does not explicitly convey information about its location. Instead, lateral localization predominantly relies on two binaural cues: the interaural time difference (ITD) and the interaural level difference (ILD). The former is based on the delay of signals between the two ears. That is, for sound source locations on the ipsilateral side of the head sound waves are delayed at the contralateral ear due to the longer travel distance, thereby creating a difference in the arrival time of the signal between the two ears. Such difference can be computed by a neural coincidence mechanism [4]. The ILD, on the other hand exploits the fact that high frequency sounds coming from the contralateral side are attenuated by the head and thereby are reduced in their intensity on the ipsilateral side [5]. The amplitude difference is computed by comparing the different intensity levels of the left and right ear.

The superior olivary complex, a midbrain region that connects the cochlear nucleus (CN) and the inferior colliculus (IC), is the first stage in the auditory pathway that receives inputs from the ipsilateral and contralateral ear and thereby is the first region of binaural processing. Particularly the lateral side of the superior olive (LSO) receives excitatory input form the ipsilateral CN and inhibitory input from the ipsilateral medial nucleus of trapezoid body (MNTB), a relay station for signals coming from the CN of the contralateral side. That is, for a high intensity signal at the ipsilateral ear, LSO

neurons are strongly excited. However, if the intensity of the signal at contralateral ear becomes stronger, the inhibition on LSO neurons is increased and their activity reduced. By integrating these signals neurons in the LSO compute the ILD between the two ears [6–8].

From the stiffness change of hair cells in the cochlea to noise suppression in the auditory cortex, the auditory system implements several adaptation mechanisms throughout its pathway. Recent investigations indicate that also the process of binaural signal integration in the LSO complex is highly dynamic and facilitated by a dedicated mechanism that allows it to rapidly adapt to statistics of perceived stimuli. Thereby providing a dynamic encoding of perceptual auditory space, which allows to maintain high sensitivity to sound source locations [9–12].

Here, we investigate adaptation ability of LSO model neurons to perceived stimuli statistics. These neurons exhibit two distinct adaptation mechanisms: an implicit and explicit one. The former emerges from the sensitivity of LSO neurons to differences of signal arrival time [6]. The physiological nature of this mechanisms allows it to work instantly. The latter one is realized by a retrograde GABA signaling pathway [13] and works in the magnitude of seconds.

By adapting to recently perceived stimuli, the (neural) system potentially improves its localization precision for consecutive stimuli, since it is likely that two consecutive sounds originate from nearby spatial locations. In other words, adapting to a previous stimulus can increase accuracy of the consecutive one. This behavior was shown for human participants in a behavioral experiment in which they had to localize sound sources after being exposed to an adapter tone [9, 14]. In addition, the authors conducted neurophysiological experiments with gerbils that led them to the hypothesis that this adaptation is due to a "retrograde GABA signaling pathway" that inhibits the afferents of an LSO neuron and thereby adapts the neuron's responses based on its recent activity.

How these adaptation mechanisms could be realized in a canonical framework of neural models and to what extend they support and even improve the localization of sound sources is investigated in the following. The implemented neural model serves as an example on how such an adaptation mechanism can be realized in a canonical framework with the potential to take place in other tasks where synaptic adaptation is required. Simulations indicate that this adaptation enables a large increase in the effective operational range while simultaneously providing higher resolution of the spatial location of interest in the perceptual auditory space.

We develop a computational model of the neural dynamics for adaptive shift estimation in binaural sound localization which supposedly takes place in the LSO complex. The model neurons utilize conductance-based properties of state change from excitatory and inhibitory inputs. Fast adaptation is achieved by a local control mechanism based on an activity dependent GABA pathway which adapts the effective synaptic integration at the basal dendrites of LSO neurons.

A series of computational experiments are reported to investigate efficacies of various adaptation mechanisms of model neurons and to quantitatively analyze their functionalities. First, the model response to a default set of interaural level differences is presented and model parameter influence on the response is investigated. It demonstrates how the input weighting determines the resolution and extend of ILD encoding. Experiment two introduces an adaptation mechanism based on a dynamical weighting of synaptic inputs and for the first time, provides a quantitative analysis of the adaptation efficacy of LSO neurons thereby providing a means for further evaluation of adaptation mechanisms. Experiment three explores the influence of the dynamical weighting on stimulus statistics and demonstrates how this introduced adaptation mechanism reacts to changing input stimulus statistics providing a higher resolution for

locations of interest. Another adaptation mechanism is investigated in experiment four, demonstrating model responsiveness to the difference of input signal arrival time. In the final experiment, model performance is tested under real world conditions demonstrating the ability of the model to reliably encode ILD of recorded natural sounds.

Model

In this section we introduce the architecture of the model which components and interactions are based on neurophysiological findings. The LSO complex is the first stage of binaural processing in the auditory pathway. It receives direct ascending inputs from spherical bushy cells (SBC) of the ipsilateral CN and indirect inputs from globular bushy cells (GBC) of the contralateral CN, via the MNTB. The MNTB serves as a relay station that converts the excitatory signal of GBC neurons to an inhibitory input to the LSO. In contrast, SBC neurons of the ipsilateral CN project directly to the LSO and provide excitatory input. By integrating these two signals, neurons of the LSO encode the ILD by means of a monotonic correspondence between response rate and ILD of the signal. Taken into account this physiological hierarchy the presented model consists of these two distinct neuron populations and their circuit-level interactions as shown in Fig. 1.

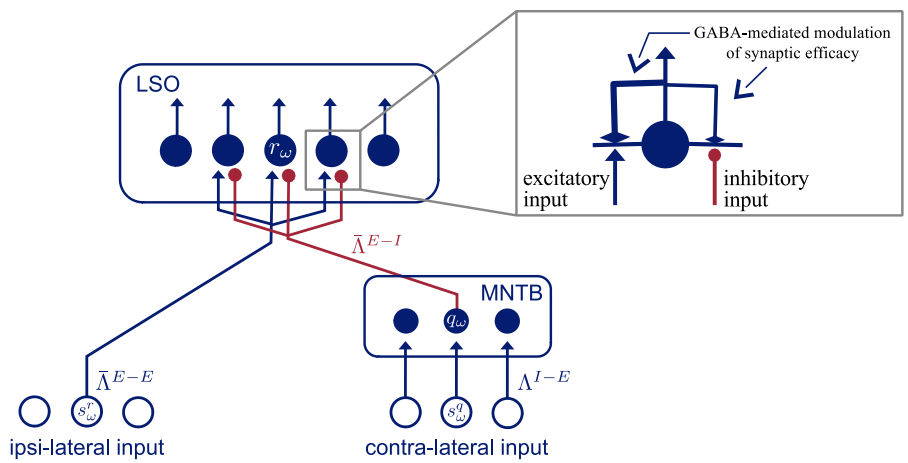

Fig 1. Architecture of model. Blue filled circles represent model neurons. Blue empty circles indicate inputs to the model neurons. Red arrows are inhibitory and blue arrows are excitatory connections from inputs to neurons and neurons to other neurons, respectively. Box at top right corner is a enlarged view on the synaptic connections of an LSO neuron. The output of an LSO neuron modulates its afferent connections.

Each of these populations comprises an array of N neurons, each selective to a specific frequency band centered at frequency ω (the neuron's characteristic frequency). Their response is formally described by a first-order ordinary differential equation of the change of its membrane potential (see [15, 16]). The input conductances to a modeled LSO cell are defined by s^r_ω and s^q_ω. These inputs represent the activity of SBC and GBC cells of the ipsi- and contralateral CN, respectively, with characteristic frequency $\omega = \{1, ..., N\}$. Thereby inputs to the model as well as the neurons within a population are tonotopically ordered. The input signals to the model are assumed to emerge from neuron populations of preceding stages of the LSO in the auditory pathway, namely spherical and globular bushy cells in the ipsi- and contralateral cochlear nucleus, respectively. It has been shown that the activity of these cells is a linear function of the sound level in dB (logarithmic scale) of perceived stimuli [8]. For simplicity, it is thereby

assumed that the inputs are in the range $s_\omega^{\{r,q\}} = [0,1]$ and that the values linearly correspond to the perceived level intensities.

LSO neurons

The modeled LSO neuron population receives excitatory input from SBC cells and inhibitory input from neurons of the MNTB population. The membrane potential r_ω of an LSO neuron, selective to frequency band ω is modeled by

$$\tau_r \dot{r}_\omega = -\alpha_r r_\omega + (\beta_r - r_\omega) \cdot \sum_{\omega'} s_{\omega'}^r \bar{\Lambda}_{\omega\omega'}^{E-E} - (\gamma_r + \kappa_r r_\omega) \cdot \sum_{\omega'} g_q(q_{\omega'}^r) \bar{\Lambda}_{\omega\omega'}^{E-I} \tag{1}$$

where s_ω^r describes the ipsilateral excitatory input to an LSO neuron, arising from an hypothetical input population of SBC neurons and weighted by an interaction kernel of excitatory to excitatory, $E-E$, connections $\bar{\Lambda}^{E-E}$. It is sufficient to directly take the value of s_ω^r as the input without transferring it by an activation function. The parameter τ_r defines the membrane capacity, α_r is a passive membrane leaking rate, β_r describes a saturation level of excitatory inputs and γ_r and κ_r define the subtractive and divisive influence of the inhibitory input, respectively. The inhibitory input q_ω is passed through its activation function $g_q(x)$ and weighted by an interaction kernel of inhibitory to excitatory, $E-I$, connections $\bar{\Lambda}^{E-I}$.

The key feature of the model is a retrograde GABA signaling circuit [13] that attenuates the efficacy of the model's afferent connections, where the individual effectiveness depends on the activity of a single LSO neuron. This adaptive inhibition is asymmetric exerting stronger inhibition on excitatory synaptic input than on inhibitory synaptic input. To account for these effects, we incorporated an activity-dependent modulation function that decreases the effective weight coefficients. Formally, we replace the weight kernels Λ_ω^{E-E} and Λ_ω^{E-I} by state-dependent adaptive terms

$$\bar{\Lambda}_{\omega\omega'}^{E-E} = \Lambda_{\omega\omega'}^{E-E} \cdot (1 - \lambda_E p_\omega) \tag{2}$$

and

$$\bar{\Lambda}_{\omega\omega'}^{E-I} = (\Lambda_{\omega\omega'}^{E-I} + \delta_r) \cdot (1 - \lambda_I p_\omega), \tag{3}$$

respectively. The parameter δ_r denotes an offset level for inhibitory GABA signaling strength and λ_E and λ_I are the GABA receptor effectivenesses on the excitatory and inhibitory input, respectively. We will discuss these parameters and their origin in more detail in section GABA Parameter Strength. The state variable p_ω models the GABA receptor activation over time and can be described by

$$\tau_p \dot{p}_\omega = -\alpha_p p_\omega + (\beta_p - p_\omega) \cdot r_\omega \tag{4}$$

where parameter τ_p defines the membrane capacity, α_p is a decay rate and β_p describes a saturation level of the inputs. The net effect of this weight adaptation in the kernels is a monotonic reduction of the efficacy of the excitatory and inhibitory inputs of an LSO neuron. The down-modulatory effect on the effective weights is controlled by the activity of the LSO neuron itself. This mechanism allows the neuron to adapt to stimulus history and thereby provide a means for dynamic adaptation.

The firing rate of an LSO neuron is calculated by a sigmoidal activation function g_r of its membrane potential r_ω

$$g_r(r_\omega) = \frac{1}{(1 + \exp(-(r_\omega - b) \cdot a))} \tag{5}$$

MNTB neurons

Model MNTB neurons receive excitatory input from GBC of the contralateral CN and project an inhibitory signal to the ipsilateral LSO [17]. Thereby, MNTB neurons are a relay station between the ipsi- and contralateral hemisphere. The inhibitory input q_ω from relay cells in the MNTB to the LSO complex is defined by

$$\tau_q \dot{q}_\omega = -\alpha_q q_\omega + \beta_q \cdot \sum_{\omega'} s^q_{\omega'} \Lambda^{I-E}_{\omega\omega'} \tag{6}$$

where s^q_ω describes the contralateral input to an MNTB neuron, arising from an input population of GBC neurons and weighted by interaction kernel $\bar{\Lambda}^{I-E}$. Parameters τ_q, α_q and β_q have same functionality as in eq. *1*. The interaction kernels of the neuron inputs in eq 1 and 6 are normalized Gaussians with different sigmas $\sigma^i, i \in \{E-E, E-I, I-E\}$ depending on the given connection (see table 1).

The firing rate of an MNTB neuron is defined by the rectified signal of its membrane potential

$$g_q(q_\omega) = [q_\omega]_+ = max(q_\omega, 0) \tag{7}$$

Table 1. Model parameters

General Parameters			
N (# Neurons)	5		
sigmoid parameter a	20		
sigmoid parameter b	0.2		
LSO Neuron			
τ_r	0.05	λ_I	1.0
α_r	1.0	λ_E	2.0
β_r	1.0	σ^{E-E}	0.5
γ_r	2.0	σ^{E-I}	0.6
κ_r	3.0	δ_r	0.16
MNTB Neuron			
τ_q	0.25	σ^{I-E}	0.1
α_q	2.0		
β_q	1.0		
GABA Receptor			
γ_p	25.0		
α_p	10.0		
β_p	10.0		

Table 2. Adapted parameters for real world stimuli

LSO Neuron	
σ^{E-E}	2.5
σ^{E-I}	3.0
MNTB Neuron	
σ^{E-E}	0.5

Results

Model simulations in this section provide a basis for evaluating binaural stimulus integration and a quantitative analysis of the adaptation efficacy of model neurons simulating LSO functions.

In a first experiment general response properties of the model under different neuron parameter conditions are presented. We show that the response range and the coding precision of model neurons can be adjusted by altering parameter values that control how inhibitory inputs are integrated to calculate the membrane potential. Having demonstrated that, we introduce a retrograde GABA signaling circuit to the model that dynamically alters the effective strength of the inhibitory inputs based on recent neuron activity.

Thus, the second experiment inspects the response adaptation for this local GABA inhibition circuit. The strength of the inhibitory GABA signals imposed on the excitatory and inhibitory inputs determines the efficacy and shape of the adaptation. By systematically varying parameters that control the strength of the inhibitory GABA signals, an optimal value for the ratio of the parameters is identified on the basis of a novel adaptation index. This adaptation index (similar to the *standard separation* in [18] and [14]) quantifies the coding precision of a neuron with respect to its ability to register relative (azimuthal) offsets of sound sources, thereby creating a unique measure of the adaptation quality. This index is the basis for evaluation and comparison of the different adaptation processes and efficacies in the following experiments.

The effect of the introduced adaptation mechanism on response characteristics based on stimulus history is examined in experiment three. Here, the influence of stimulus history on location estimation is measured by presenting adapter tones with fixed ILDs shortly followed by test stimuli with different ILDs, similar to behavioral experiments in [14] and [9].

Experiment four characterizes a second adaptation process in LSO neurons: the influence of time delays between the ipsilateral and contralateral inputs on the adaptation capacity of the model neuron. It demonstrates that the offset of arrival time between the input signals plays a crucial role in the integration process and facilitates higher localization accuracy.

To test the validity and performance of the model, real world stimuli are presented that are recorded in a sound attenuated chamber from different locations on the horizontal plane, ranging from $-90°$ to $90°$ azimuth. Model responses are compared to analytically calculated ILDs that serve as ground truth. We demonstrate that the model is able to successfully compute the ILD of real world stimuli.

All in the following presented results are calculated from the network responses readout at a single neuron level after keeping the input stimuli constant for at least 400 time steps. This duration is sufficient for the neuron to dynamically converge to its equilibrium membrane potential of numerical integration of the state equations (see Fig. 3 inset).

In particular, a constant level is presented for 400 time steps to the ipsilateral and contralateral input populations before changing it. This presentation time corresponds to the reaction time of neurons and is consistent throughout all experiments expect experiment number 4. For the numerical integration of the state equations we chose *Euler's method* with a step size of $\Delta t = 0.001$ (for details see [19]).

The choice of model parameters of the neurons is crucial for their response behavior in terms of the effective response range (steepest slope) and of the range of dynamic adaptation. The parameters for the following simulations are chosen to fit a variety of neurophysiological experiments. In particular, we focused on the results of the dynamic adaptation experiment [13] (experiment 2 and 3), where they demonstrate that activation of a retrograde GABA signaling pathway leads to a shift of LSO neurons'

response curves, and the input timing experiment [6] (experiment no. 4), in which it is shown that LSO neurons respond to the ITD of the presented signals.

Parameter influence and response behavior

Typically, neural models have several parameters (e.g. membrane capacity, leaking rate) that can be tuned to achieve a desired response behavior of a model neuron. Since we are investigating the integration of two incoming signals, the most influential parameters are the ones that control the effective strength of those signals on the membrane potential.

Therefore, the first experiment investigates the influence of model parameter values that control the influence and strength of inhibitory inputs. We demonstrate that the typical response curve of LSO neurons (sigmoidal function over ILDs) is shifted and that its slope is modulated by these parameters. In addition, the experiment shows the *default response* of a single LSO neuron that is used for comparison in further experiments. Since the purpose of this experiment is to investigate influence of model parameters without the influence of dynamic adaptation, GABA receptor parameters λ_E and λ_I are set to 0, effectively disabling this retrograde GABA signaling circuit.

Input stimuli to the neuron model over time are shown in Fig. 2. Ipsi- and contralateral inputs are presented as monotonic functions of the sound level over time (decreasing for ipsilateral input and increasing for contralateral input, respectively). These input functions have several plateaus i.e. constant levels over time that allows the neuron's membrane potential to reach a steady state (see Fig. 3 inset). Note, that the response of a single LSO neuron is the result of a dynamic process of direct excitatory inputs and indirect inhibitory inputs from MNTB neurons.

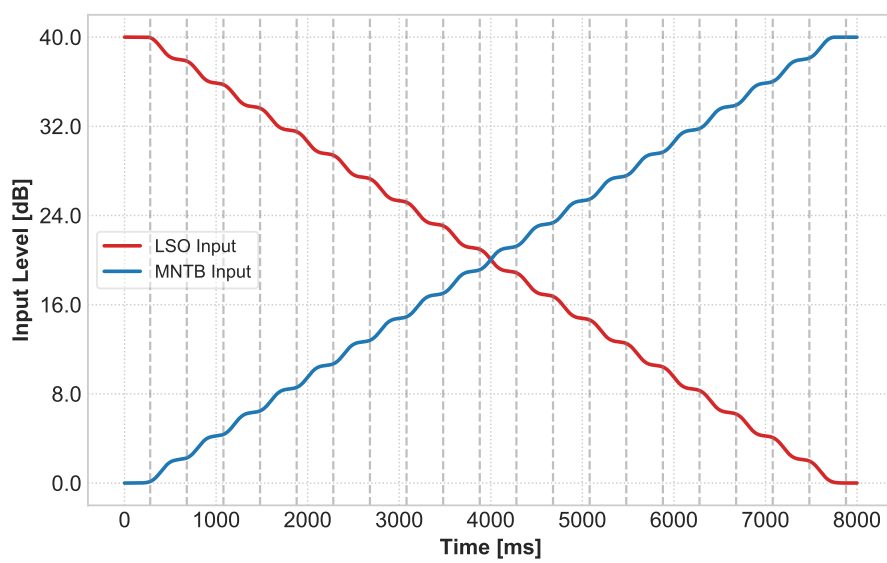

Fig 2. Input generation for the model system for ILD calculation. Red line shows excitatory input from cells of the ipsilateral cochlear nucleus to LSO neurons. Blue line shows excitatory input from cells of the contralateral cochlear nucleus to MNTB neuron which are converted to inhibitory input to LSO neurons. Vertical grey dashed lines indicate measurement points of neuron's response.

The output response of a model LSO neuron is computed by applying a sigmoid transfer function (see Eq. 5) to the membrane potential to generate a firing rate. The transfer function is tuned to have typical response properties of measured neurons in

mammals [6, 20]. The observed output response of LSO neurons starts to increase for slightly negative ILD values, which corresponds to a louder sound at the contralateral ear and has its steepest slope for positive ILD values before it saturates for a maximal perceivable ILD value (in this model $40dB$). The response of the model for the default set of parameter values, as defined in table 1, is shown in Fig. 3.

Since the maximal numerical input to our model neuron is scaled to be positive and lower than 1.0, the range of input level difference is $[-1.0, 1.0]$ (i.e. an input value of 1.0 on the ipsilateral and an input value of 0.0 on the contralateral side and vice versa). We defined the range of perceivable ILD to be between $40dB$ and $-40dB$ to be in line with physiological ILD values [21, 22].

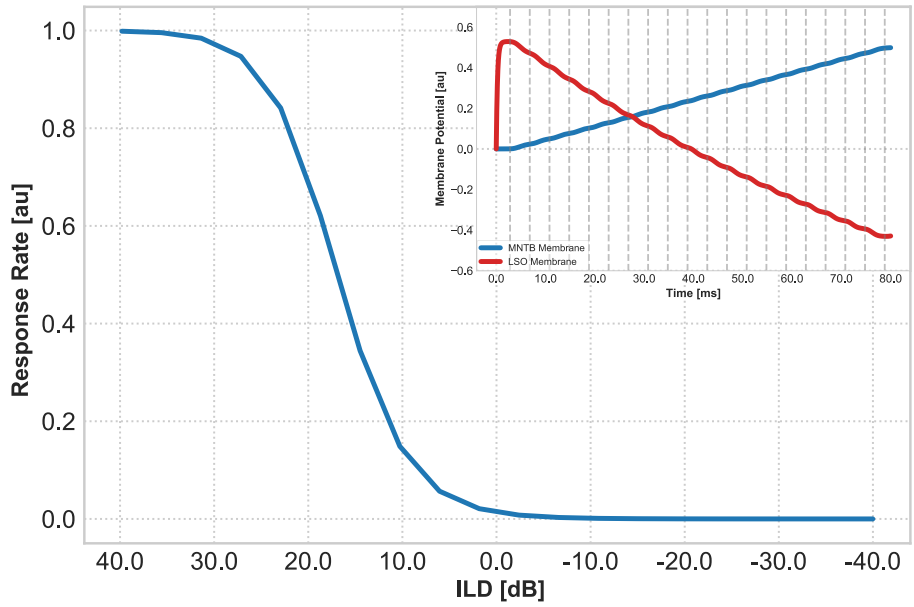

Fig 3. Model response of an LSO neuron for default set of parameter values. Blue line shows the response rate of a single LSO neuron to stimuli as presented in Fig. 2 over interaural level difference. The ILD is determined by subtracting the level of the ipsilateral stimulus from the level of the contralateral stimulus. Inset shows membrane potentials for LSO (activity r, red) and MNTB (activity q, blue) neurons. Probing times (grey dashed lines) are chosen to ensure that both membrane potentials have reached a steady state before measuring. These states can be identified by horizontal plateaus in the display where the membrane potential is constant.

Two major mechanisms of gain control in neuronal circuits exist: *shunting* and *subtractive inhibition*. The term shunting refers to its effect of locally reducing the input resistance and increasing its conductances, thereby reducing the amplitude of excitatory postsynaptic potentials (EPSP) [23]. Subtractive inhibition is achieved by hyperpolarization of the neuron's membrane due to the opening of voltage gated potassium channels.

Figure 4 displays the influence of the LSO membrane equation parameters γ_r (upper plot) and κ_r (lower plot) (Eq. 1) that define the effect and type of the inhibitory input on the membrane potential. In the present model the parameter κ_r controls the strength of the shunting term. The algebraic solution of the steady-state response of this inhibition type results in divisive inhibition. For $\gamma_r = 0, \kappa_r > 0$ the inhibition becomes a pure shunting inhibition. The strength of subtractive inhibition can be controlled by the parameter γ_r and for $\gamma_r > 0, \kappa_r = 0$ the inhibitory input operates in a pure subtractive manner. When $\gamma_r > 0, \kappa_r > 0$ the inhibitory input is a combination of

both inhibition mechanisms (see [16] for more details on parameter influence).

The displayed responses are attained by keeping one of the parameters at its default value ($\gamma_r = 2$ and $\kappa_r = 3$) while varying the other. Plot **A** of Fig. 4 displays the difference in response behavior for varying γ_r values. Increasing this parameter simultaneously leads to a steeper slope and a shift of the point of complete suppression towards positive ILD values (louder tone at ipsilateral ear). By that, it is possible to define the effective response range of the neuron. Plot **B** of Fig. 4 depicts the response for different κ_r values. The slope of the response function is similar over all presented values. Also the point of zero response stays constant. The only noticeable change is in the effective operating point, i.e. the point at which the neuron is maximally sensitive to changes. For small κ_r values this point is closer to $0dB$ and shifts towards positive ILDs for larger values. We choose the values of the parameters to resemble neurophysiological response characteristics of LSO neurons. That is, a maximal response close to the maximal perceivable difference and a point of zero response close to $0dB$ with a maximal sensitivity for sounds coming from the ipsilateral side.

The effect of the two parameters can also be seen in displays of the membrane potential (Fig. 4 insets), where parameter κ_r defines whether the function decays in a convex or concave manner. The point of zero crossing does not change for different parameter values. In contrast, parameter γ_r changes the slope of the function (steeper slope for higher values) and by that shifts the point of zero crossing. The shape of the function however remains linear.

As proposed in [21] neural dynamics together with their thresholds are not the only factors that can determine the neuron's response behavior. Also stimulus latencies play a crucial role as shown in the next experiment.

Dynamic adaptation of response behavior

Experiment two and three investigate the neural basis for dynamic adaptation in simulations of modeled LSO neurons. Recent neurophysiological findings revealed that neurons in the LSO employ a synaptic adaptation circuit that facilitates the neuron to adapt to recent stimulus history. This circuit has functional implications for sound localization as it shifts the range of highest sensitivity of the neuron towards recently perceived stimulus locations [9, 13, 14]. The underlying principle of this synaptic circuit is the activation of pre-synatipc GABA receptors which regulate the effectiveness of excitatory and to a lesser extend inhibitory inputs. This mechanism depends on the activity of the LSO neuron itself and is in contrast to other gain control mechanism [24] not regulated by higher level (feedback) projections.

In their experiments with gerbils [13] Magnusson and colleagues applied the $GABA_b$ receptor agonist Baclofen during sound stimulation and measured the response rate of single LSO neurons. The application of Baclofen suppressed the response of the neuron compared to measurements before application of the drug (Fig. 1 in [13]). To inspect the location of such inhibition the investigators conducted further in vitro experiments with brain stem slices. These experiments confirmed that the inhibition takes place at the pre-synaptic connection by modulating the transmitter release. This leads to an attenuation of the connection strength and facilitates a gain control mechanism. Our model implements such a mechanism by means of an activity dependent reduction of excitatory and inhibitory input strength (see Eq. 2 and 3). The following experiments investigate the effect of the retrograde GABA signaling and its influence on stimulus history, by (i) systematically varying the effectiveness of the signal imposed on the excitatory and inhibitory input, respectively (see Fig. 6), and (ii) by measuring the influence of a preceding adapter tone on consecutive stimuli as in [14] and [9] (see Fig. 8).

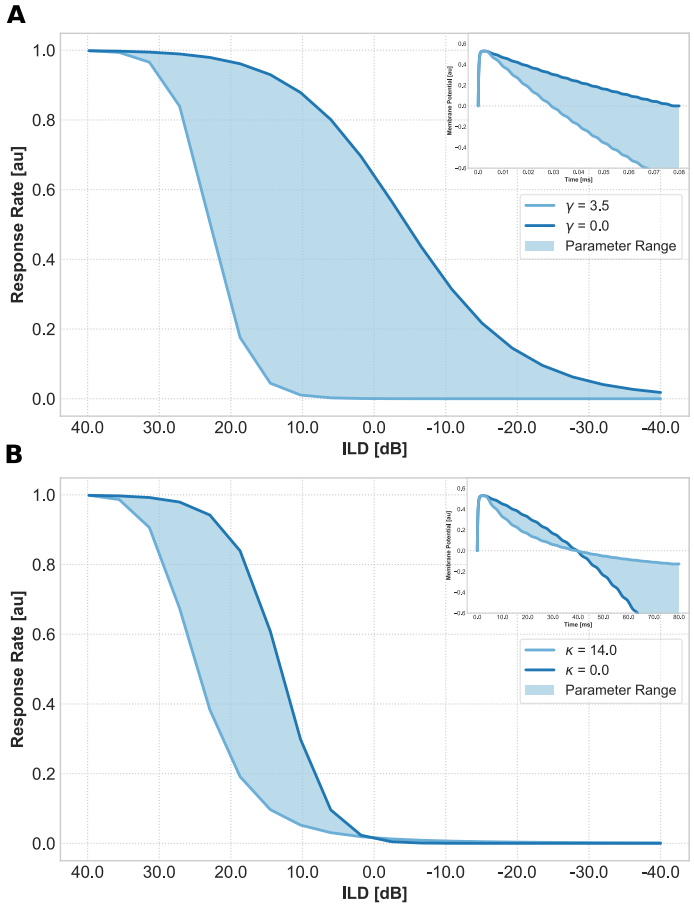

Fig 4. Model response for parameter values γ_r, κ_r Plot **A** displays model responses for varying γ_r values in range $[0.0, 3.5]$ that control the strength of subtractive inhibition. Plot **B** shows model responses for different κ_r values in range $[0.0, 14]$ that regulates the effect of shunting inhibition on the membrane potential. Filled areas are approximated from simulation results.

GABA Parameter Strength In their study [13], the authors report that the response curve of an LSO neuron is shifted towards more positive ILD values for activated $GABA_b$ receptors (as shown in Fig. 7). Two possible processes are conceivable that facilitate a shift of the response function towards positive ILD values: one is an increasing effect of the inhibitory input and therefore a greater suppression of the LSO neuron. However, $GABA_b$ is known as an inhibitory transmitter and it is therefore unlikely to enhance inputs. The second, more likely, process suggests the suppression of the excitatory input which leads in turn to a greater influence of the inhibitory input. As a consequence, the response function is shifted towards more positive ILDs. The authors argued that the influence of the $GABA_b$ receptor activation on the excitatory and inhibitory inputs of the neuron differs and has a stronger effect on the excitatory projections.

To verify their argument, we investigate the response of a model LSO neuron for an inverse ratio of $GABA$ receptor effectiveness ($\lambda_e < \lambda_i$). That is, we increase the effectiveness of $GABA$ inhibition on the inhibitory inputs and reduce it on the excitatory inputs. This interaction leads to a more broadly tuned response function (see Fig. 5). This is contradictory to neurophysiological findings where $GABA_b$ receptor

activation leads to a finer tuning of the response curve. For our model we can conclude that in order to exhibit similar responses as measured in vitro, the effectiveness of $GABA$ on the inhibitory inputs needs to be stronger ($\lambda_e \geq \lambda_i$). This is in line with results of in vitro experiments [13]. However, it is possible that the neural system takes advantage of this effect to increase the perceivable range of the LSO neuron (see Discussion for further details).

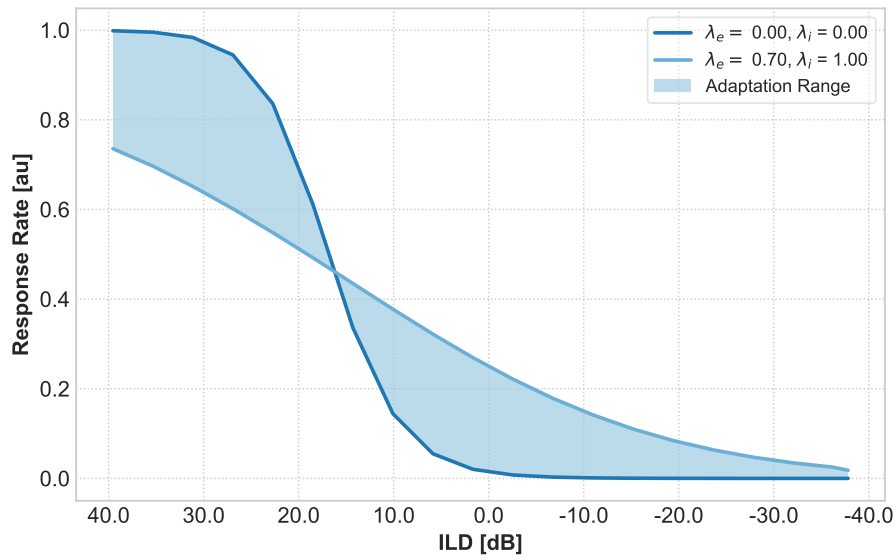

Fig 5. Adaptation range of model LSO neuron for inverse $GABA_b$ receptor effectiveness. Parameters λ_e and λ_i describe the inhibition effectiveness on excitatory and inhibitory inputs respectively. Normal (dark blue line) and shifted (light blue line) responses are shown. For $\lambda_e = \lambda_i = 0$ the ILD response curve is the same as the default response (Fig. 3 and no dynamic adaptation process takes place. For $\lambda_e = 0.70$ and $\lambda_i = 1.0$ (inverse ratio) the response curve's slope and consequently its sensitivity is decreased while the perception range is increased.

As shown in Fig. 5, the GABA inhibition on the inhibitory input needs to be stronger to have the observed effect on LSO neurons (as presented in [13]). However, how much stronger the effect of GABA on the inhibitory input compared to the excitatory input needs to be to achieve an optimal adaptation to stimuli statistics is unknown.

Thus, experiment 2 explores the optimal ratio of the $GABA$ inhibition efficacies on the inputs. This is achieved by an exhaustive parameter evaluation in which it is assumed that an optimal ratio entails maintaining a preferably high *coding precision* over the entire adaptation range. The *coding precision* is a measurement index adapted from the standard separation between two stimulus values and is defined as the derivative of the neuron's response curve. In contrast, the standard separation is defined by the difference of the firing rate of the two stimuli divided by the geometric mean of their standard deviations (see [13, 25, 26] for details). High coding precision values indicate steep slopes in the response curve of the neuron which, in turn, describe a high sensitivity of the neuron to changes in ILD values. Figure 6 depicts coding precision values for all parameter combinations $\lambda_E, \lambda_I \in [0, 1]$. Black dots indicate peaks in the coding precision for given λ_E and λ_I values and create a straight line with slope 0.5 and intercept 0.16 when interpolated. These values are used as an indication for the GABA effectiveness on the inputs. We can conclude that the optimal ratio of $GABA$ effectiveness on excitatory and inhibitory inputs in terms of coding precision is $1 : 2$. Consequently, we choose model parameters so that the efficacy of $GABA$ on the

inhibitory input is twice as high as for the excitatory input ($\lambda_E = \lambda_I \cdot 2$) with an initial offset of $\delta_r = 0.16$.

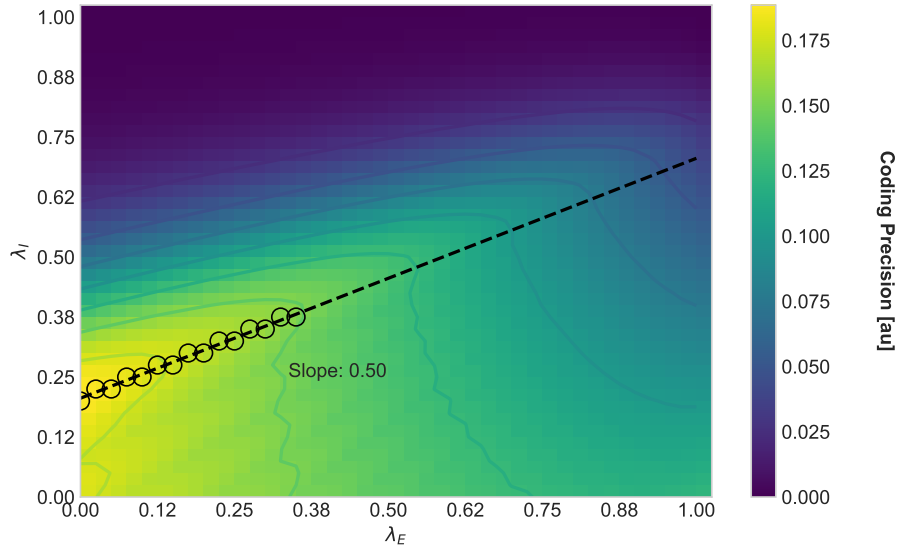

Fig 6. Exhaustive parameter evaluation of the $GABA$ parameters λ_E, λ_I . Each point in the heat map indicates the coding precision value for a certain combination of λ_E (abscissa) and λ_I (ordinate). We assume that the neuron's task is to achieve a preferably high coding precision value. Black dots depict these values (the maxima of the map). A linear function was fitted to those points (linear regression) and the slope ($m = 0.50$) and bias ($b = 0.16$) calculated.

The adaptation of the ILD response function for these parameters is depicted in Fig. 7. For increasing parameter values the excitatory and inhibitory inputs are gradually inhibited which consequently shifts the ILD response function (blue area). The values $\lambda_e = 0.72$ and $\lambda_i = 0.36$ indicate the maximally effective inhibition since for higher values the response function did not shift further but remained constant. We take that as an indication for the maximal adaptation range facilitated by this gain control mechanism.

Neural adaptation to stimulus history The third experiment tests the effect of the introduced gain control mechanism on localization quality. Previously conducted psychophysical experiments indicate that human subjects adapt to the history of recently presented stimuli [9, 14]. In a first study the human participants were tested with a $1s$ adapter tone of various ILD, consisting of broadband noise and an average binaural level of $60dB$, followed by a 100 ms target tone of a constant ILD value over time [14]. The participants then had to indicate, in a two-alternative forced-choice task, whether the target sound was perceived on the left or right side of the midline ($0dB$ ILD). Results show that the perceived midline of participants shifts in direction of the previously perceived adapter tone. The authors hypothesized that this is due to the effect that the brain attempts to maintain high sensitivity for locations of high stimulus density (here, the location of the previously perceived adapter tone). In addition, they report a response adaptation of neurons in the inferior colliculus (IC) of ferrets stimulated with a similar stimulus set as the human participants. Whether this adaptation process is constrained to IC neurons or takes place in a preceding processing stage, namely the LSO, was not investigated in this study. However, another study investigated neurons in the medial superior olive (MSO) for their adaptation capabilities

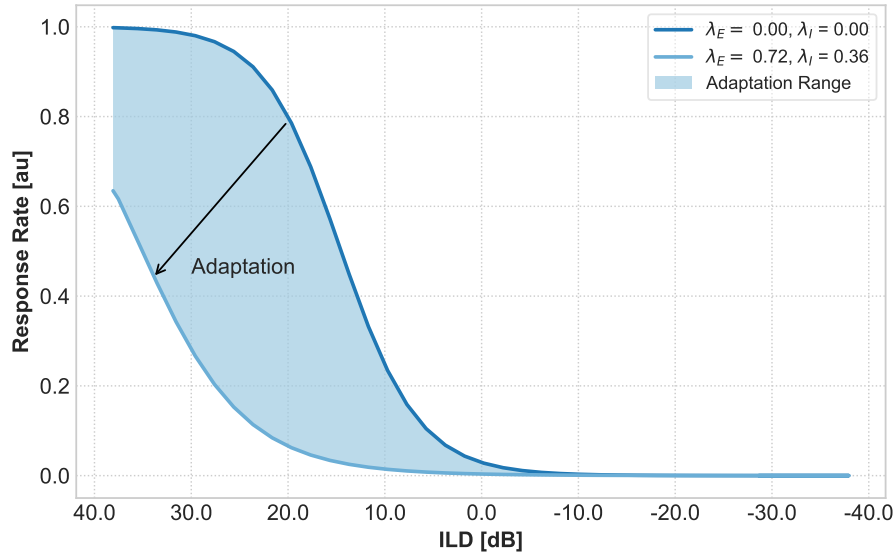

Fig 7. Adaptation range of model LSO neuron for increasing parameter values. The parameters λ_e and λ_i describe the inhibition strength on excitatory and inhibitory inputs respectively. Normal (dark blue line) and shifted (light blue line) responses are shown. For $\lambda_e = \lambda_i = 0$ the ILD response function is similar to the default response and no dynamic adaptation process takes place. The light blue area indicates the adaptation range.

to perceived sounds with different ITDs [27] and found similar adaptation capabilities.

Likewise, Lingner and colleagues [9] presented human participants with three different adapter tones ($1s$ duration,0 µs, -181.4 µs or 634.9 µs ITD) followed by a target tone with different ITDs ranging from -634.9 to +634.9 µs. All presented sounds have a frequency of $200Hz$. The authors reported a perceived shift of the target stimuli away from the adapter tone, indicating that the perceptual auditory space around the adapter tone is widened, leading to a higher sensitivity of sounds with ITDs similar to the adapter tone.

Taken together, the results of these studies demonstrate that the auditory system adapts dynamically to ILD and ITD on a behavioral level and comprises retrograde GABA signaling mechanisms in principal areas that process ITD and ILD information. However, whether LSO neurons exploit their retrograde GABA signaling mechanism to adapt to ILDs of previously perceived stimuli has not yet been shown. We hypothesize that this adaptation processes take places at the level of the LSO by retrograde signaling of GABA transmitters as described in [13]. To test this hypothesis, the following experiment investigates the effect of stimulus statistics on model LSO neurons and their retrograde GABA signaling circuit. As in [14], an adapter tone is presented that is followed by a stimulus of various input level intensities. We expect that a preceding adapter tone activates the retrograde GABA circuit which attenuates the model's response magnitude of the subsequent stimuli. Therefore, shifting the response of the LSO neuron towards the ILD of the adapter tone.

The stimulus arrangement for this experiment is shown in Fig. 8. It comprises an adapter tone of $1.2s$ with temporal ramps at the beginning and end of the sound followed by a $500ms$ period of silence. Subsequently, the target stimulus is presented with a duration of $2s$ and an ILD within the range as defined below. There are 41 adapter tones and 41 test stimuli of different level intensities. Hence, a total number of $41 \times 41 = 1681$ unique stimulus arrangements are presented to the model. The level

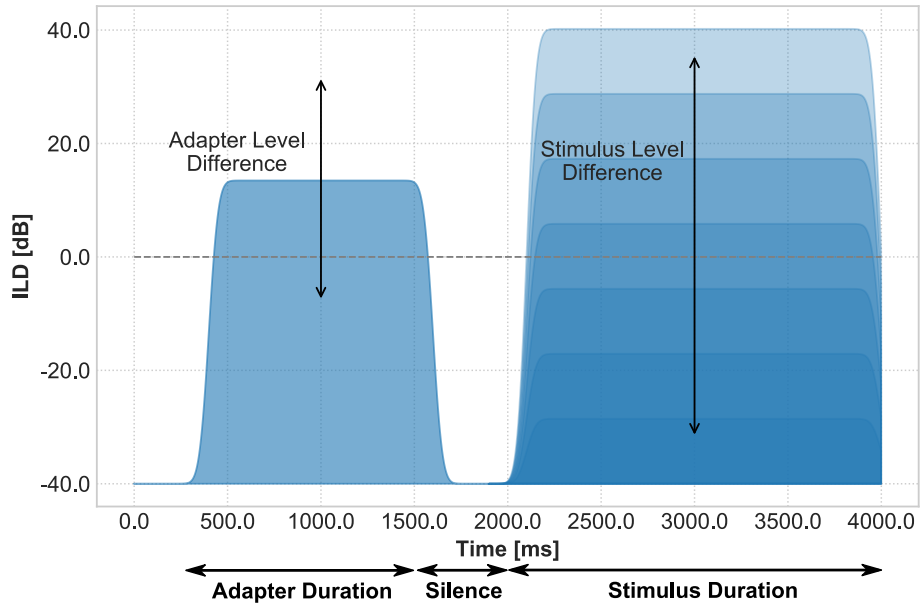

Fig 8. Input stimulus example for Experiment 4. The first ridge depicts the ILD of the adapter tone with a duration of $1.2s$ followed by a break of $500ms$. The second ridge shows the ILD of the actual test stimulus. Differently shaded areas illustrate different test stimulus ILDs for the same adapter tone. Grey dashed line marks $0dB$ ILD.

intensity of an adapter tone as well as a test stimulus ranges from $-50dB$ to $50dB$. Adapter tones are added and subtracted to the base line intensity of $50dB$, on the contra- and ipsilateral side, thereby creating ILDs of $-100dB$ and $100dB$, respectively. For example, an adapter tone of 0 ILD indicates a sound level of $50dB$ on both sides whereas negative adapter tone levels decrease the input level on the contralateral and increase it on the ipsilateral side.

Responses of the LSO neuron model over time for three different adapter tone ILDs ($100dB, 50dB, 0dB$) and a constant test stimulus ILD of $100dB$ are shown in Fig. 9. This test setup corresponds to a scenario in which the adapter tone source is varied between three different locations (90°, 45° and 0° azimuth) on the ipsilateral side and the test stimulus is located on the very far ipsilateral side (90° azimuth). The preceding adapter stimulus activates the retrograde GABA signaling circuit which subsequently attenuates the effectiveness of the neuron's inputs. The response to the adapter tone stimulus accurately follows the input to the model. However, the response to the target stimulus (between $2000ms$ and $2500ms$) is attenuated based on the ILD of the preceding adapter tone. As a consequence, this adaptation is leading to a shift of the model's response curve towards the ILD of the adapter tone, as depicted in Fig. 10. Measurements of the neuron activity are taken $260ms$ after stimulus onset to measure the initial response of the neuron. This elapse time was chosen because after the initial response the retrograde GABA circuit (p_ω) is affected by the more recent activity of the neuron and the effect of the adapter tone vanishes. This is due to the time constant (τ_p) of the adaptive term of the GABA circuit (see Eq. 4). For adapter tones with negative ILDs, i.e. located at the contralateral side, no adaptation takes place (the response is similar to the default response of the neuron) since the adapter tone's ILD does not evoke a considerable activation of the GABA circuit of simulated neurons of the ipsilateral hemisphere. However, adapter tones with positive ILDs, i.e. located on the ipsilateral side, sufficiently excite the neuron to activate the GABA circuit (increasing

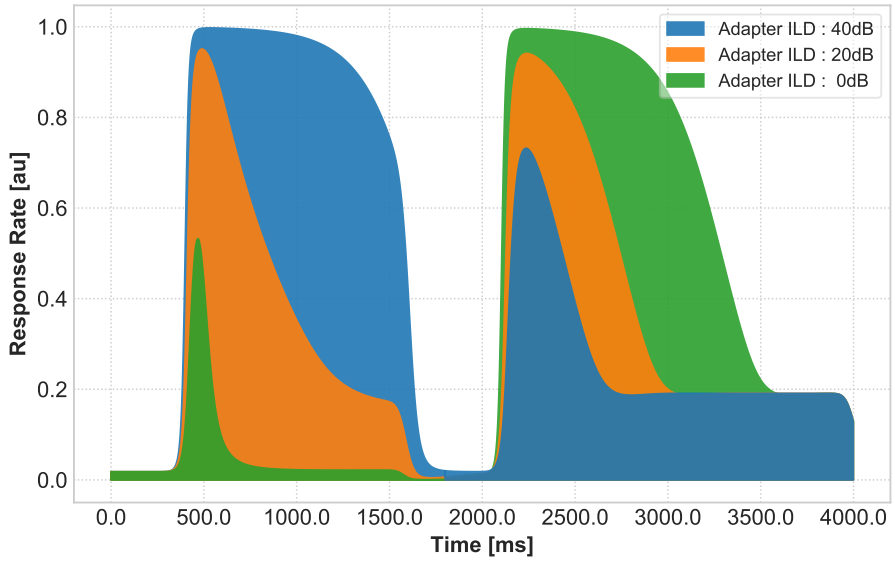

Fig 9. Responses of model neuron to different adapter tone intensities (blue $100dB$, orange $50dB$, green $0dB$) and constant test stimulus intensity ($100dB$). The response of the neuron to an adapter tone sound level of $100dB$ (blue line) is maximal. However, the responses to the consecutive test stimuli is reduced through adaptation i.e. the higher the ILD of the adapter tone the lower the response to the test stimulus.

value of p_ω in membrane equation). Consequently, such adapter tones decrease the effectiveness of the inputs (by modulating the input weight kernels $\Lambda^{E-E}_{\omega\omega'}$ and $\Lambda^{E-I}_{\omega\omega'}$ of the excitatory $(E-E)$ and inhibitory $(E-I)$ inputs, respectively, see Eq. 2 and 3) which leads to a response shift. In other words, the neuron's response curve and consequently the region with the steepest slope, thus highest sensitivity, shifts towards the adapter tone. This leads to a higher sensitivity of consecutive sounds of the same ILD.

Timing

A binaural stimulus simultaneously creates a time and level difference of its sound signal at the sensory level where the relationship between those two cues is monotone (considering broad-band stimuli): Increasing the ITD of a stimulus monotonically decreases the ILD of this stimulus and vice versa. For example, a sound source located at the ipsilateral side of the head produces not only a higher sound level but also a delay of signal arrival time at the contralateral ear. The nature of ILD processing, that is the timed interaction of excitatory and inhibitory inputs, already leads to an essential sensitivity to the arrival time of the inputs. Neurophysiological studies support this in showing that neurons in the LSO are not merely responsive to the level difference but are also sensitive to differences of arrival time of the excitatory and inhibitory inputs [6, 7, 28]. To test to what extend the present model reacts to stimuli with various ITDs, how this leads to adaptation and to compare its adaptation effectiveness to the previous adaptation mechanisms, the fourth experiment investigates the influence of signal arrival time on model neurons response characteristics.

Network response of a model neuron for stimuli with varying ILDs over ITDs is depicted in Fig. 11. A negative ITD refers to a sound source located on the ipsilateral side of the head, i.e. it arrives at the ipsilateral side first and therefore leads to a delay of

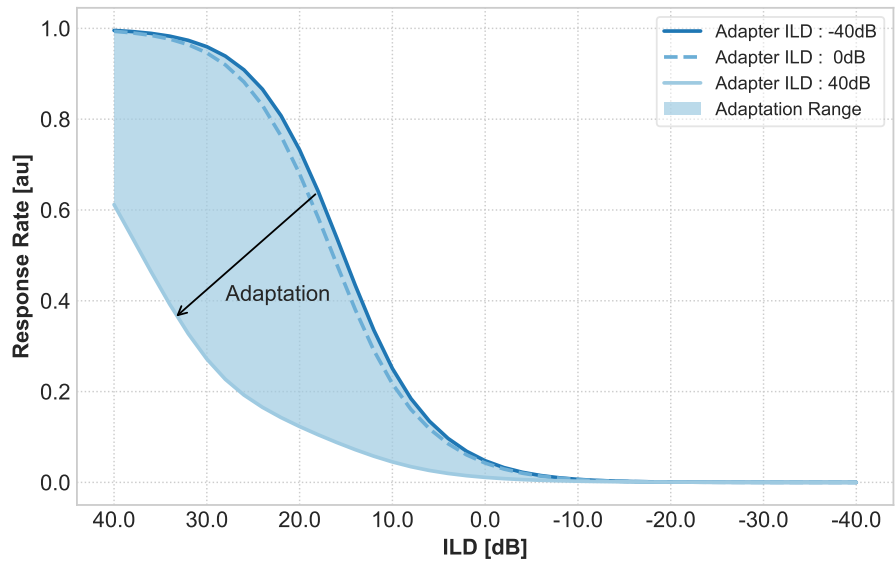

Fig 10. Response of a single LSO neuron to stimuli of constant ILD after the presentation of various adapter tone ILDs. Light blue dashed line depicts the response to a test stimulus of ILD $100dB$ after presenting an adapter ILD of $0dB$. Dark blue line draws the response to the same test stimulus after presenting an adapter ILD of $-100dB$. No adaptation takes place and the response is similar to the default response of the neuron (compare Fig. 3). Light blue line draws the attenuated response to the same test stimulus after presenting an adapter ILD of $100dB$.

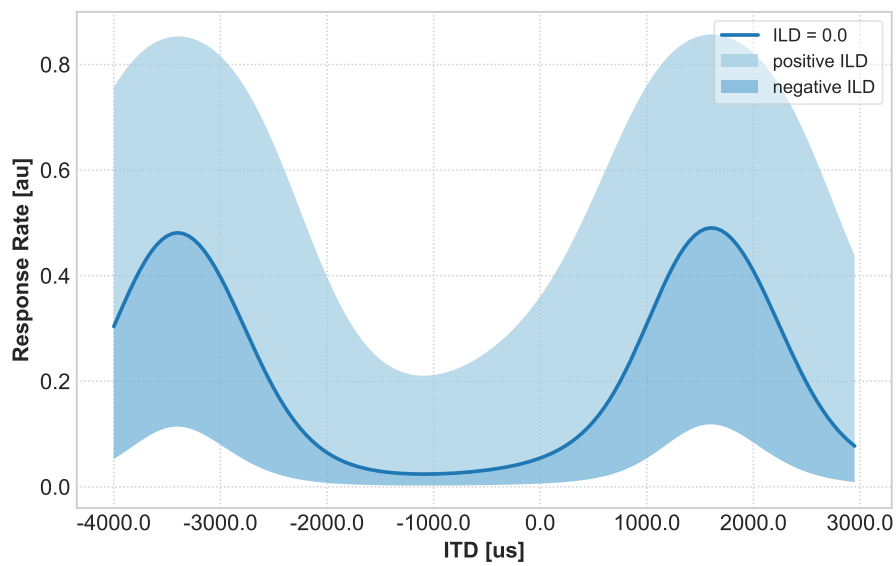

Fig 11. Responsiveness of LSO neuron for different ILDs over ITDs. The blue line indicates the neuron response for $0dB$ level difference, the darker blue area shows possible responses for higher ILD values, whereas the light blue area indicates possible responses for negative ILD values. The depicted ILD range is limited to $-36dB$ and $+36dB$ for a clearer plot.

the contralateral signal. The effectiveness of an inhibitory input on an excitatory input is decreased for larger time delays between the two input signals, i.e. the excitatory input might be already processed before the other arrives and vice versa. In concert with neurophysiological results, the response of the model LSO neuron strongly depends on the ITD value of the incoming signal (see [6] Fig. 3 for comparison). For ITDs around $-1500\,\mu s$ the delayed arrival of the inhibitory input signal causes a reduction of its effectiveness on the response rate. Only inhibitory signals with high level intensity generate a noticeable effect. In contrast, for ITDs around $1000\,\mu s$ the inhibitory signal arrives even before the excitatory signal and leads to a-priori depolarization of the membrane potential. Thus, already low level inhibitory signals cause a reduction of the response rate. This results in a u-shaped response curve, in contrast to a v-shaped response curve for negative ITD values as reported in [22]. As natural stimuli with negative ITDs essentially exhibit positive ILDs and vice versa, the shift in the response rate indicates an adaptation towards more relevant input ranges. In other words, the interaural time difference affects the sensitivity of the neuron for ILDs by means of changing the inhibitory input effectiveness. This process is an inherent adaptation since it is caused by stimulus statistics and not by a dedicated neural mechanism.

In order to investigate the effect of this adaptation, Fig. 12 depicts the response curves of a simulated LSO neuron for stimuli with various ITD values over ILD. The outer boundaries of the filled area indicate model responses to ITDs ($-1000\,\mu s$ and $1500\,\mu s$) for which the response curve is shifted maximally and thus delimits maximal adaptation. For higher or lower ITDs the response curve is shifted between those maximal values. The shift of the response is maximal $8dB$ for stimuli located at the far ipsilateral side and maximal $32dB$ for stimuli on the far contralateral side. Shifting the response curve facilitates a higher sensitivity to changes in the ILD of the input signal and indicates an adaptation to the perceived stimulus. The limited shift towards positive ILDs results from maximal effectiveness of the inhibitory input. That is, the inhibitory input leads to a maximal strength of the hyperpolarization for only a specific ITD (in this case $-1000\,\mu s$). For stimuli with higher or lower ITDs the hyperpolarization effect vanishes. The larger extend of the rightward shift of the response curve results from a decreasing effectiveness of the inhibitory input. This leads to a lowering of the activation threshold of the neuron. The extend of the rightward shift depends on the intrinsic model parameters (compare Fig. 4). For an ITD of $1500\,\mu s$ the inhibitory input signal arrives too late, no longer having a noticeable effect on the response. Hence, the neuron's response curve solely depends on the level intensity of the excitatory input signal.

For better visualization, Fig. 13 displays the receptive field of an LSO neuron with respect to ITD and ILD values in 2D.

Here, the range of ITD values is chosen to demonstrate the maximal adaptation effect of the stimulus. However, note that naturally occurring ITD values for humans are in the range of $[-600\,\mu s, 600\,\mu s]$ (see S19 Figure). For this smaller range of ITDs the increase of adaptation precision is still $6db$.

The fact that loud signals are transmitted faster, i.e. they exhibit shorter transduction delays, supports the shift of the response curve towards a more relevant range [22]. However this was not modeled explicitly.

Another process that facilitates a shift of the response curve to a great extend towards positive ILDs is by means of GABA inhibition of the afferent connections. We investigate this in the following experiment.

Real world stimuli

To demonstrate the robustness of the model and its response behavior to real world stimuli, it is probed with real world recordings of different sound types in this last

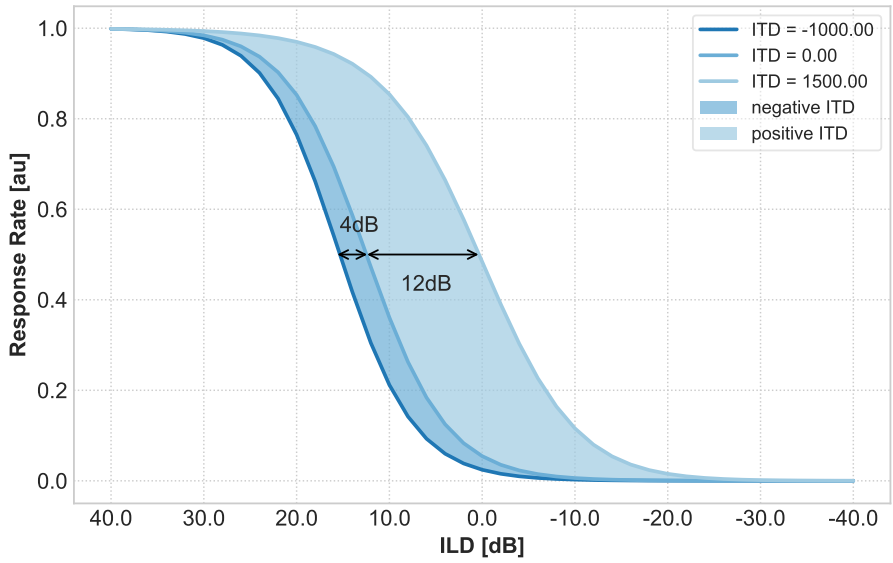

Fig 12. Adaptation range of model LSO neuron for various ITDs of the input signals. Light blue line and corresponding filled area indicates model response for stimuli with positive ITDs. Dark blue area shows responses for stimuli with negative ITDs. Area filled with blue is inferred from simulation results.

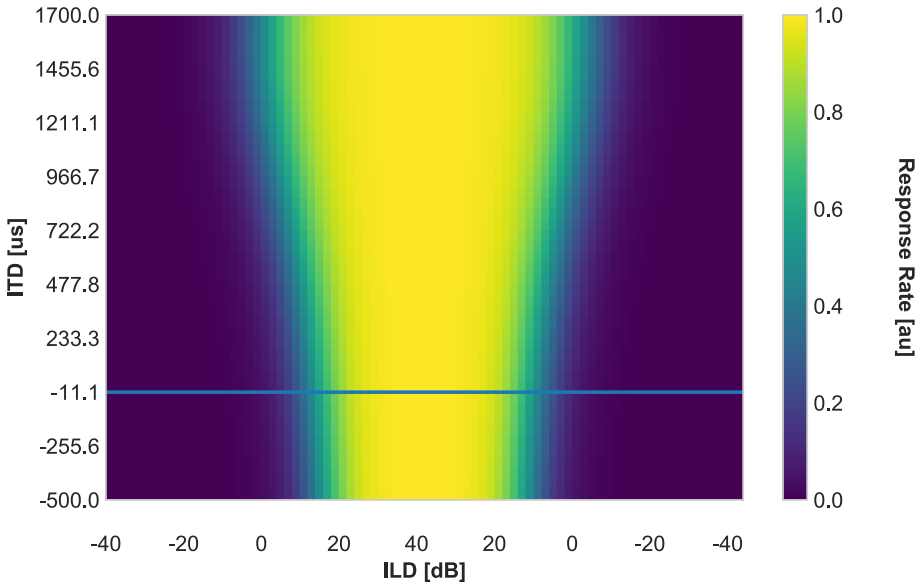

Fig 13. Receptive field of model LSO neuron for input stimuli with various ITD and ILD value. The blue line indicates an ITD of 0 µs. Note that the plot is mirrored at $100dB$ ILD for better visualization of the receptive field.

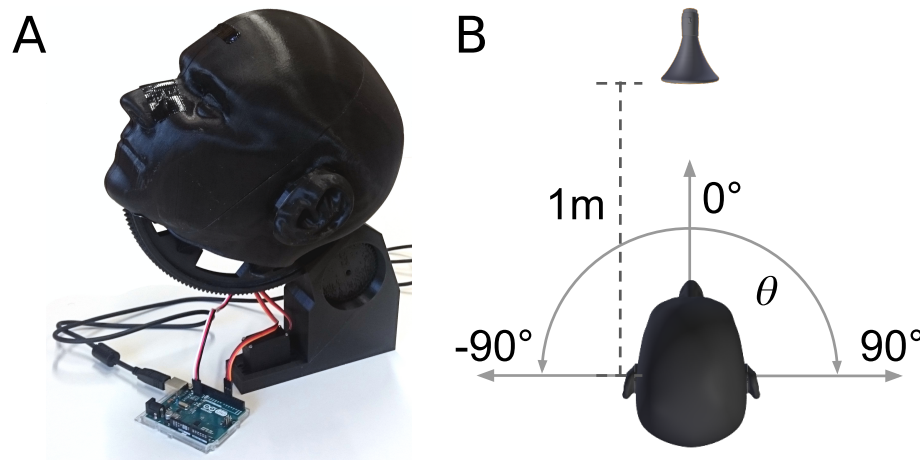

Fig 14. Device and setup for real world sound recordings. A shows the 3D printed, anatomical correct replication of a human head and ears. In the ears, approximately $2cm$ inside the ear canal, standard microphones are placed for recording. The head is controlled by two servo motors, one for turning around the longitudinal axis (azimuth), the other for turning around the frontal axis (elevation). All sounds are recorded for 0° elevation (head facing the speaker) and different azimuth directions. **B** shows the setup for the recordings. The head is centered $1m$ in front of a standard speaker and can rotate around its longitudinal axis from $\theta = -90°$ to $\theta = 90°$ with a minimal step increment of 1°.

experiment. Sounds are recorded with two standard microphones placed inside the right and left ear canal of human-like shaped ears on a dummy head as depicted in Fig. 14 **A**. The device can turn around its longitudinal axis to create a relative displacement of the sound source location in the horizontal plane. The distance to the speaker (standard speaker) remains constant (1m) during movement (Fig. 14 **B**). The presented sound types comprise monaurally recorded real world sounds, e.g. a dog barking, clapping hands, a gun shot or a vacuum cleaner. We tested 10 different sound types to cover a wide range of different spectra. Each sound type was presented for azimuthal head directions of $[-90, -70, -50, -30, -10, 10, 30, 50, 70, 90]°$ and 0° elevation. Each sound is played back from the speaker and recorded in stereo with the two in-ear microphones for the duration of the sound. All recordings were done in a sound attenuated room. The recorded signals were then presented to our model. To obtain a biologically plausible input to the model a gammatone filter bank [29] was applied separately for signals recorded from the right and left microphone, respectively. As a result, the signals are transformed into a spectrogram with 24 frequency bands with the energy normalized, over all frequency bands and time. These bands are then used as an input to our model, which for this experiment comprises 24 neurons simulating LSO functions and 24 neurons simulating MNTB functions, respectively. Recorded signals from the left microphone serve as the ipsilateral input s^r_ω of model LSO neurons, whereas the contralateral input s^q_ω to model MNTB neurons is given by the recorded signal of the right microphone. The kernel sizes of the input kernels are increased as a function of frequency to match the number of frequency bands (see Table 2).

The energy content of the 24 frequency channels over time for a white noise stimulus is shown in Fig. 15. For this plot the head is turned to azimuth $-90°$ so that the sound is perceived from the ipsilateral side. Part **A** shows the excitatory after the gammatone filter bank transformation is applied, Part **B** the inhibitory input, respectively. The strength of the two input signals differs with an ipsilateral input level on average $14dB$

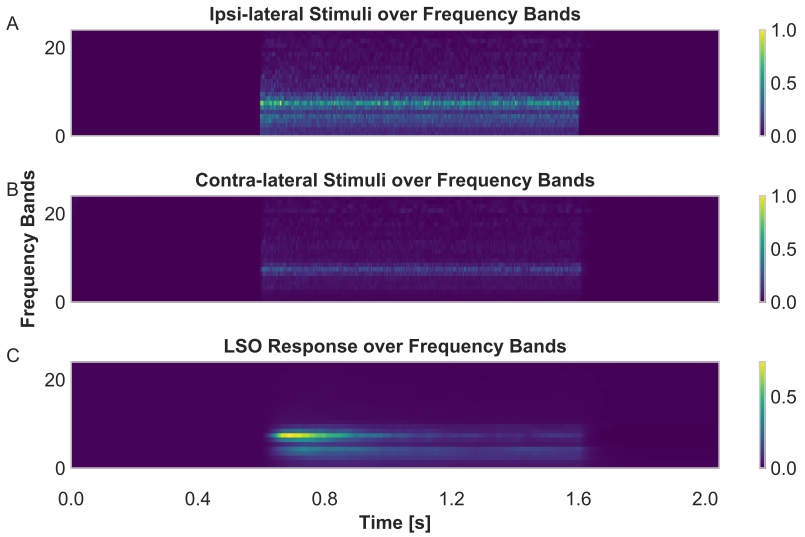

Fig 15. Input Signal after gammatone filter transformation. Plots **A** and **B** show the input to the model LSO and MNTB neuron, respectively. The signal is binned in 24 frequency bands over time. Plot **C** shows the response (r_ω) of the model LSO neuron over time. The presented stimulus was Gaussian white noise with a duration of $1s$ with $0.5s$ of silence before and after the stimulus.

higher than the contralateral input level. Part **C** shows the model LSO neuron response over time for the given input. About 0.5 s after stimulus onset neurons in the frequency band primarily activated (in this case no. 7) reached their steady state and showed a constant response. At this time the average response over all frequency bands was calculated. We will refer to this value as the overall response of the model system and use it to display ILDs for different head directions.

The mean response over all sound type recordings is shown in Fig. 16. To compare the quality of the localization ability of our model, the averaged and normalized ILD of the recordings is plotted in the same graph (dashed black line). The model response follows the actual ILD value of the recordings accurately. We can conclude that our model is capable of encoding the ILD of perceived sound signals accurately and could be used in real world applications.

Discussion

We introduced a conductance-based model simulating functions of LSO and MNTB neurons for the encoding of ILD values. To evaluate the model we used simulated as well as real world sounds. The model incorporates a novel synaptic modulation mechanism that facilitates dynamic adaptation to stimulus statistics.

In Experiment 1, we demonstrated the effect of model parameters γ_r and κ_r on the response behavior of a model neuron. Specifically we showed that, the subtractive inhibition parameter γ_r controls the response range of the neuron whereas the shunting inhibition parameter κ determines the slope of the response. These findings indicate that the neuron's membrane dynamics need to comprise a balanced combination of subtractive and shunting inhibition in order to cover a wide range of input ILDs while simultaneously maintaining a high sensitivity (see Fig. 18). This is important for the adaptation of LSO neurons since it demonstrates that the response curve of neurons can

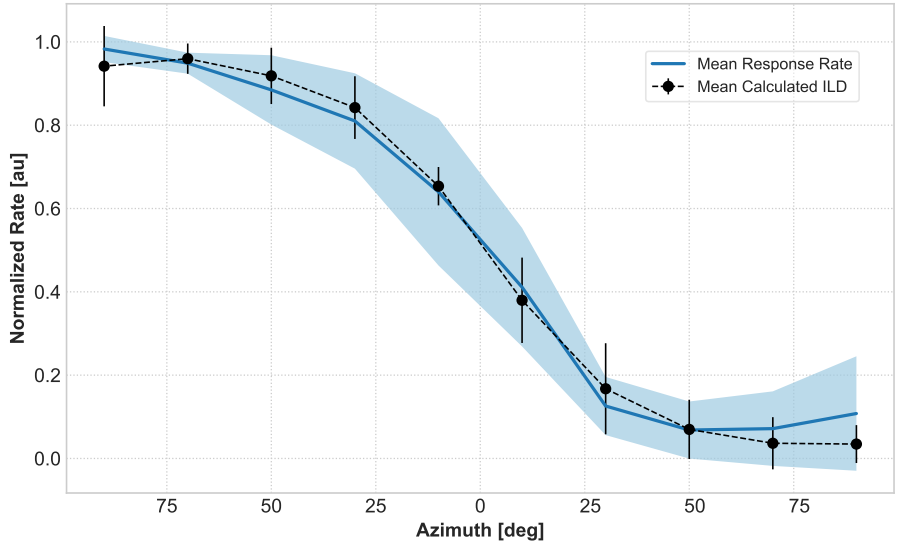

Fig 16. Mean model response for all presented sound types. Blue line is the mean response of the model. Light blue area indicates the standard deviation of the response. Mean response rate of the ILD of all sound types, calculated from the real world recordings together with the standard deviation is shown (dashed black line).

be controlled by the way the inhibitory input is integrated. Therefore, we hypothesis that the retrograde GABA circuit might have various impact on the subtractive and divisive integration process of a neuron.

The ratio between the effectiveness of GABAergic inhibition on the excitatory and inhibitory inputs, respectively, is a crucial factor to ensure high coding precision of neurons as demonstrated in Experiment 2. Only a higher effectiveness on the excitatory input than on the inhibitory input leads to a response shift towards more relevant input range. However, based on the results presented in Fig. 5, we propose that an inverse ratio of the GABAergic inhibition on the inputs can lead to an extension of the neuron's response range with a reduction in its sensitivity based on the coding precision index (derivative of the neuron's response curve, high values indicating high sensitivity of the neuron to changes in ILD values, see section GABA Parameter Strength). This would enable a single neuron to tune its response for a wide range of input stimuli. However, adaptation always comes with a trade-off. In this case, the trade-off is between the ability to respond to a wide range of stimuli and the achieved coding precision.

The two presented adaptation mechanisms are very different in their underlying principles, however, yield the same effect: adaptation of the response based on stimulus statistics. To quantitatively assess the quality of the adaptation process, we introduced the coding precision value. Based on this index we can now compare the two adaptation processes based on their sensitivity gain and the extend of the response shift (see Fig. 17). The presented coding precision values are similar to the ones measured in gerbils (Fig. 8 in [14] when presented with a similar adapter-stimulus combination.

The adaptation induced by the retrograde GABA circuit leads to a shift of $22dB$ of the coding precision maximum towards the ILD of the adapter tone, which corresponds to a gain in sensitivity for ILDs close to the adapter. Particularly, the amplitude of the coding precision and consequently the slope of the response curve at these ILDs is increased by at least 97% of its original value, i.e. when no adaptation takes place. In contrast, the adaptation induced by different arrival times of ipsi- and contralateral stimuli (Experiment 4, blue lines) indicates a shift of $16dB$ towards the contralateral

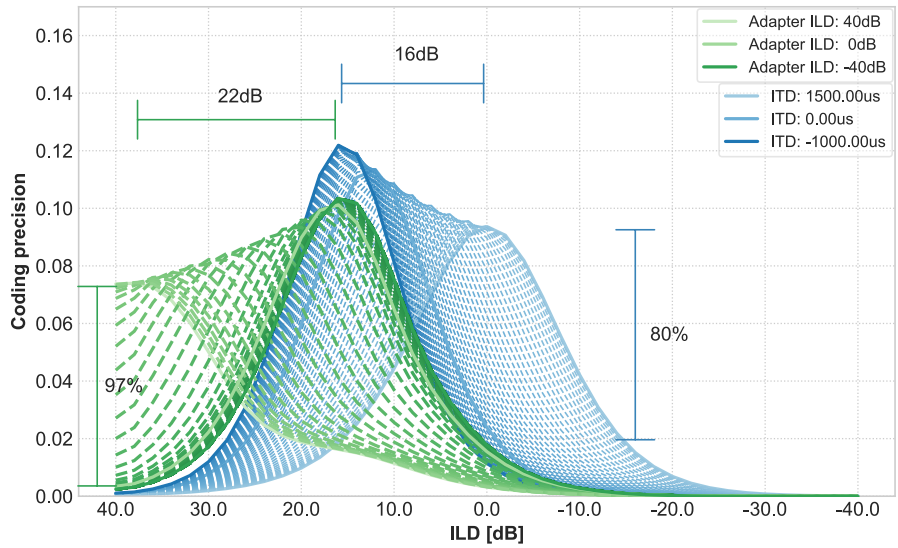

Fig 17. Comparison of coding precision between GABA and ITD induced adaptation. Green lines indicate the coding precision of the adapter tone experiment (no. 4). The peak of the coding precision curve is shifted by a maximum of $22dB$ for increased adapter tone intensity and gains an sensitivity increment of 97%. Blue lines depict the coding precision of the timing experiment (no. 4). The peak of the coding precision curve is shifted by a maximum of $16dB$ between stimuli of different ITDs. The increment of sensitivity for this shift is 80%.

side and gains 80% of its original sensitivity.

These response shifts can be explained by a reduction or enhancement of the effectiveness of the excitatory and inhibitory inputs depending on the underlying adaptation processes. The reduction is achieved explicitly by inhibiting the excitatory and inhibitory inputs through dynamic temporal adaptation of the weight kernels $\Lambda^{E-E}_{\omega\omega'}$ and $\Lambda^{E-I}_{\omega\omega'}$. As a consequence, the operational range of the membrane potential (maximal value of r_ω) is reduced which leads to a decreased activation ($g_r(r_\omega)$) of the neuron. In other words, for the same stimulus ILD the neuron exhibits a lower activation level, hence the response over ILD is shifted. In contrast, the enhancement is caused implicitly by a temporal delay of the inhibitory input signal which leads to a reduced influence of this signal in the integration process with the excitatory input signal.

The difference in the maximum of the coding precision function between the adapted and the non-adapted condition is due to the dynamics of the model neuron. If no adaptation takes place the saturation of the membrane potential of the neuron is reached for an ILD of $40dB$. However, if the GABA circuit attenuates the effectiveness of the inputs, the saturation point of the membrane potential is never reached. Hence, the neuron's membrane potential is constantly below the saturation point for all input ILDs and can not reach it's default activation level. In the case of temporally delayed input signals, the inhibitory input exerts less influence which has a similar effect as increasing parameter values κ_r and γ_r (parameters to define the strength of the inhibitory influence). As can be seen in Fig. 4 the change of the inhibitory influence strength changes the slope of the response function. A decreased slope in the ILD response functions leads to a lower amplitude of the coding precision function. Together, the sensitivity to ITD and the retrograde GABA signaling circuit enable a flexible encoding of auditory space and extend the input range of a neuron significantly ($22dB + 16dB = 38dB$).

The presented adaptation mechanism of retrograde GABA signaling on the example of LSO neurons is very simplistic, thus, is likely to take place in other domains of signal integration. For example, neurons in the medial superior olive complex integrate ipsi- and contralateral signals for ITD encoding and could profit from such an adaptation mechanism. Short term synaptic plasticity is a commonly found property of neurons in various brain areas. The introduced mechanism creates a canonical principal for synaptic adaptation and therefore could account for several adaptation mechanisms in the brain [30, 31].

The first and -to the best of our knowledge- the only single cell model of LSO neurons was introduced by [32] and further investigated in [33]. The authors introduced a detailed multi-compartment model of a LSO neuron which explains its spiking behavior in particular its chopper response at stimulus onset. This response behavior is of minor interest in the present study since we focused on the adaptation mechanisms of LSO neurons and the consequent implications on improved encoding of auditory space which was not the target of Zacksenhouse and colleagues in their studies.

There are several properties of the auditory pathway that are currently not considered in the design of this model, since we believe that these properties do not weaken its predictive power. Nevertheless, we will discuss several of them below that could improve the model and might be targeted in further investigations.

The inputs to the model originate from spherical and globular bushy cells in the ipsi- and contralateral cochlear nucleus, respectively. In our model, we assumed that the characteristics of these inputs are identical, both following the output of auditory nerve fibers of the ipsi- and contralateral side, respectively. That is, the activation changes linearly with the log-intensity of the input [8]. However, this might not necessarily be the case. Spherical bushy cells exhibit a strong response at the onset of a stimulus before settling on a lower response rate for the rest of the stimulus duration ("spike-frequency adaptation") [20]. In contrast, globular bushy cells' responses are almost identical to the auditory nerve input [34].

In this paper, we demonstrated how the sensitivity and range of ILD encoding in LSO neurons can be explained by model parameters. Particularly, how different inhibition types (subtractive and shunting) contribute to the response behavior of a model neuron. The neuron's responsiveness to temporal delays of its inputs indicates an inherent adaptation process which maintains high sensitivity to incoming stimuli. Together with the retrograde GABA signaling circuit, these adaptation mechanisms contribute to the high accuracy of ILD encoding in LSO neurons over a wide range of input stimuli. We compared the coding precision of the two adaptation mechanisms quantitatively and showed that an interplay between the two jointly sensitizes the circuit to enable a response shift towards contra-lateral and ipsi-lateral stimuli, respectively. Thereby a single model neuron can cover almost an entire hemisphere of auditory space. In addition, it saves computational resources by reusing the same population of LSO neurons for various ILD ranges. Most significantly, we proposed an optimal ratio between GABA effectiveness on the excitatory and inhibitory inputs, respectively. Aside the presented similarities to measured physiological responses of LSO neurons, we demonstrated the model's capability of reliable encoding of ILDs of real world sounds.

Source code

Source code of the model and all required scripts will be made publicly available on Github after publication (https://github.com/oesst/Neuron-Model-LSO).

Author contributions

TO contributed in model conception and design, experiment conduction, analysis and interpretation of data, and drafting manuscript. ME contributed in analysis and interpretation of data, and critical review. HN contributed in model conception and design, analysis and interpretation of data, and critical review.

Acknowledgments

Research conducted as part of the VA-MORPH project financed by the Baden-Württemberg foundation in the "Neurorobotik" program (project no. NEU012).

References

1. Payne RS. How the barn owl locates prey by hearing. Annu Cornell Lab Ornithol. 1962;1:151–159.
2. Knudsen EI. The Hearing of the Barn Owl. Scientific American. 1981;245(6):113–125.
3. Cherry EC. Some Experiments on the Recognition of Speech, with One and with Two Ears. The Journal of the Acoustical Society of America. 1953;25(5):975–979. doi:10.1121/1.1907229.
4. Jeffress LA. A Place Theory of Sound Localization. Journal of Comparative and Physiological Psychology. 1948;41(1):35–39. doi:10.1037/h0061495.
5. Rayleigh L. On our perception of sound direction. The London, Edinburgh, and Dublin Philosophical Magazine and Journal of Science. 1907;13(74):214–232.
6. Joris PX, Yin TC. Envelope Coding in the Lateral Superior Olive. I. Sensitivity to Interaural Time Differences. Journal of neurophysiology. 1995;73(3):1043–62. doi:10.1152/jn.1995.73.3.1043.
7. Joris PX. Envelope Coding in the Lateral Superior Olive. II. Characteristic Delays and Comparison with Responses in the Medial Superior Olive. Journal of Neurophysiology. 1996;76(4):2137–56. doi:10.1152/jn.1996.76.4.2137.
8. Joris PX, Yin TCT. Envelope Coding in the Lateral Superior Olive. III. Comparison With Afferent Pathways. Journal of Neurophysiology. 1998;79(1):253–269. doi:10.1152/jn.1998.79.1.253.
9. Lingner A, Pecka M, Leibold C, Grothe B. A Novel Concept for Dynamic Adjustment of Auditory Space. Scientific Reports. 2018;8(1):1–12. doi:10.1038/s41598-018-26690-0.
10. Keating P, Dahmen JC, King AJ. Complementary Adaptive Processes Contribute to the Developmental Plasticity of Spatial Hearing. Nature Neuroscience. 2015;18(2):185–187. doi:10.1038/nn.3914.
11. King AJ, Dahmen JC, Keating P, Leach ND, Nodal FR, Bajo VM. Neural Circuits Underlying Adaptation and Learning in the Perception of Auditory Space. Neuroscience & Biobehavioral Reviews. 2011;35(10):2129–2139. doi:10.1016/j.neubiorev.2011.03.008.

12. Park TJ, Brand A, Koch U, Ikebuchi M, Grothe B. Dynamic Changes in Level Influence Spatial Coding in the Lateral Superior Olive. Hearing Research. 2008;238(1-2):58–67. doi:10.1016/j.heares.2007.10.009.

13. Magnusson AK, Park TJ, Pecka M, Grothe B, Koch U. Retrograde GABA Signaling Adjusts Sound Localization by Balancing Excitation and Inhibition in the Brainstem. Neuron. 2008;59(1):125–137. doi:10.1016/j.neuron.2008.05.011.

14. Dahmen JC, Keating P, Nodal FR, Schulz AL, King AJ. Adaptation to Stimulus Statistics in the Perception and Neural Representation of Auditory Space. Neuron. 2010;66(6):937–948. doi:10.1016/j.neuron.2010.05.018.

15. Koch C. Biophysics of computation: information processing in single neurons. Oxford university press; 2004.

16. Brosch T, Neumann H. Computing with a Canonical Neural Circuits Model with Pool Normalization and Modulating Feedback. Neural Computation. 2014;26(12):2735–2789.

17. Smith PH, Joris PX, Yin TCT. Anatomy and Physiology of Principal Cells of the Medial Nucleus of the Trapezoid Body (MNTB) of the Cat. Journal of Neurophysiology. 1998;doi:10.1152/jn.1998.79.6.3127.

18. Wen B, Boahen K. A Silicon Cochlea with Active Coupling. IEEE Transactions on Biomedical Circuits and Systems. 2009;3(6):444–455. doi:10.1109/TBCAS.2009.2027127.

19. Süli E, Mayers DF. An introduction to numerical analysis. Cambridge university press; 2003.

20. Grothe B, Pecka M, McAlpine D. Mechanisms of Sound Localization in Mammals. Physiological Reviews. 2010;90(3):983–1012. doi:10.1152/physrev.00026.2009.

21. Park TJ, Monsivais P, Pollak GD. Processing of Interaural Intensity Differences in the LSO: Role of Interaural Threshold Differences. Journal of Neurophysiology. 1997;77(6):2863–2878. doi:10.1152/jn.1997.77.6.2863.

22. Park TJ, Grothe B, Pollak GD, Schuller G, Koch U. Neural Delays Shape Selectivity to Interaural Intensity Differences in the Lateral Superior Olive. Journal of Neuroscience. 1996;16(20):6554–6566. doi:10.1523/JNEUROSCI.16-20-06554.1996.

23. Carandini M, Heeger DJ. Normalization as a Canonical Neural Computation. Nature Reviews Neuroscience. 2012;13(1):51–62. doi:10.1038/nrn3136.

24. Shapley R. The Contrast Gain Control and Feedback Within the Retina. IFAC Proceedings Volumes. 1982;15(4):489–494. doi:10.1016/S1474-6670(17)63036-2.

25. Sakitt B. Indices of Discriminability. Nature. 1973;241(5385):133–134. doi:10.1038/241133a0.

26. Tollin DJ, Koka K, Tsai JJ. Interaural Level Difference Discrimination Thresholds for Single Neurons in the Lateral Superior Olive. Journal of Neuroscience. 2008;28(19):4848–4860. doi:10.1523/JNEUROSCI.5421-07.2008.

27. Stange A, Myoga MH, Lingner A, Ford MC, Alexandrova O, Felmy F, et al. Adaptation in Sound Localization: From GABA B Receptor-Mediated Synaptic Modulation to Perception. Nature Neuroscience. 2013;16(12):1840–1847. doi:10.1038/nn.3548.

28. Caird D, Klinke R. Processing of Binaural Stimuli by Cat Superior Olivary Complex Neurons. Experimental Brain Research. 1983;52(3):385–399. doi:10.1007/BF00238032.

29. Slaney M. Auditory toolbox. Interval Research Corporation, Tech Rep. 1998;10:1998.

30. Jääskeläinen IP, Ahveninen J, Andermann ML, Belliveau JW, Raij T, Sams M. Short-term plasticity as a neural mechanism supporting memory and attentional functions. Brain research. 2011;1422:66–81.

31. Stevenson IH, Cronin B, Sur M, Kording KP. Sensory adaptation and short term plasticity as Bayesian correction for a changing brain. PloS one. 2010;5(8):e12436.

32. Zacksenhouse M, Johnson DH, Tsuchitani C. Excitatory/Inhibitory Interaction in the LSO Revealed by Point Process Modeling. Hearing Research. 1992;62(1):105–123. doi:10.1016/0378-5955(92)90207-4.

33. Zacksenhouse M, Johnson DH, Williams J, Tsuchitani C. Single-Neuron Modeling of LSO Unit Responses. Journal of Neurophysiology. 1998;79(6):3098–3110. doi:10.1152/jn.1998.79.6.3098.

34. Niparko JK. Cochlear implants: Principles & practices. Lippincott Williams & Wilkins; 2009.

35. Irvine DR. Physiology of the auditory brainstem. In: The mammalian auditory pathway: Neurophysiology. Springer; 1992. p. 153–231.

36. Reed MC, Blum JJ. A model for the computation and encoding of azimuthal information by the lateral superior olive. The Journal of the Acoustical Society of America. 1990;88(3):1442–1453.

Supporting information

S1 Text. ILD Computation. For calculating the ILD values of real world stimuli we use the text book definition (e.g [35]) of ILD computation:

$$ILD = 10 * log_{10} \frac{\int_{t=0}^{\infty} s_l^2(t)}{\int_{t=0}^{\infty} s_r^2(t)} \tag{8}$$

where s_l is the signal received at the left ear and s_r is the signal received and the right ear at time t.

S1 Figure. Parameter influence on coding precision.

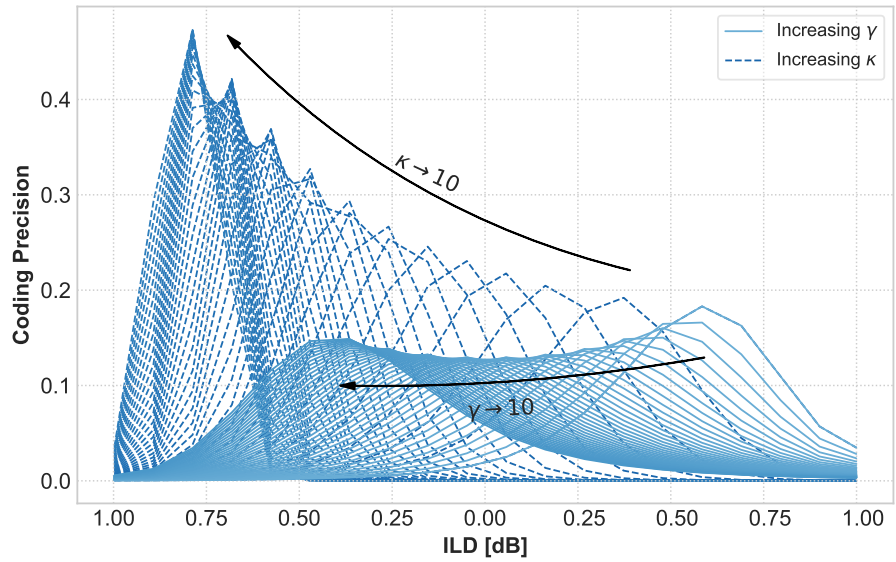

Fig 18. Parameter influence on coding precision. Dashed blue lines indicate the coding precision of the model response for changing κ parameter. For increasing parameter value the coding precision increases while simultaneously the response range decreases (the ILDs that the model exhibits a response).
Solid blue lines indicate the coding precision of the model response for changing γ parameter. For increasing parameter value the coding precision and extensions of the response range remains almost constant. However the response range itself shifts from negative to positive ILD values. A proper ratio of the two parameters facilitates a balance between high coding precision and response range.

S2 Figure. Adaptation for plausible ITD values.

S1 Text Additional experiments

Point of Complete Inhibition Park and colleagues [21] investigated properties of neurons in the LSO complex that facilitate the wide variability of ILD responses. The authors presented stimuli of different intensities to mustache bast and measured the response of individual LSO neurons. They reported that a reliable factor to compare the response behavior between neurons is the ILD of *complete inhibition* (PCI) which remains constant for a single LSO neuron but varies significantly from cell to cell

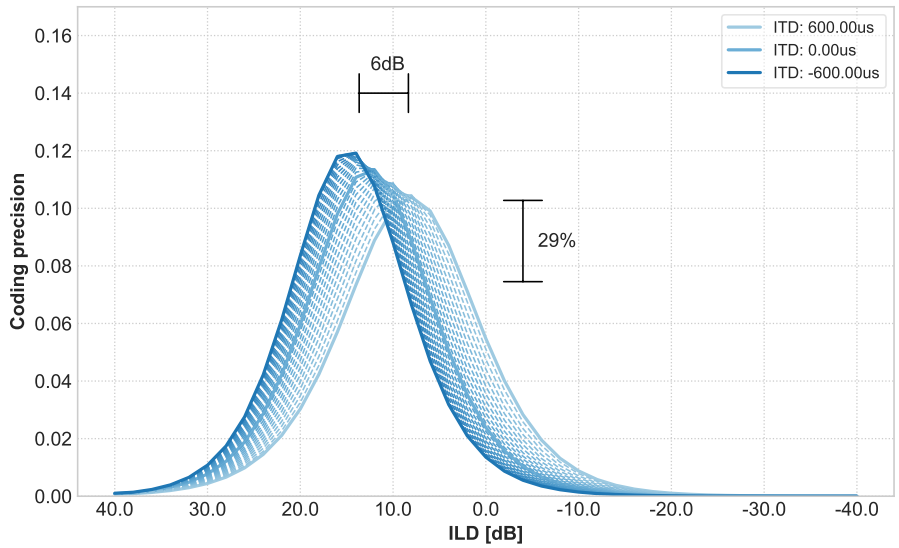

Fig 19. Coding precision for human perceivable ITDs. Blue lines depict the coding precision of the timing experiment when ITDs of stimuli are in the perceivable range of humans. The peak of the coding precision curve is shifted by a maximum of $6dB$ between stimuli of different ITDs. The increment of sensitivity for this shift is 29%

(see [21] Fig. 3). That is, the slope and maximum saturation value might differ depending on the presented stimuli level, whereas the point for which the LSO neuron is completely deactivated remains constant over different input intensities. Therefore, it can serve as a unique index to describe the neuron's response characteristic. To compare their findings with results of the present model, figure 20 (upper plot) shows the model response to similar stimuli. That is, a signal of constant level intensity is presented on the ipsilateral side (as noted in the legend) and a signal of consecutively increasing level intensity is presented on the contralateral side. The response of a model neuron varies with varying input intensities but the point of complete inhibition remains constant. This result also confirms the threshold hypothesis of Reed and Blum [36], which states that the difference of thresholds for excitatory and inhibitory input corresponds with the point of complete inhibition. That is, the effectiveness of the excitatory and inhibitory inputs on a neuron's dynamics determine its point of complete inhibition. In the presented model inhibitory thresholds can be controlled by the parameters κ and γ. As shown in fig. 4 membrane parameter values indeed change the point of complete inhibition and therefore contribute to the variety of ILD responses of LSO neurons.

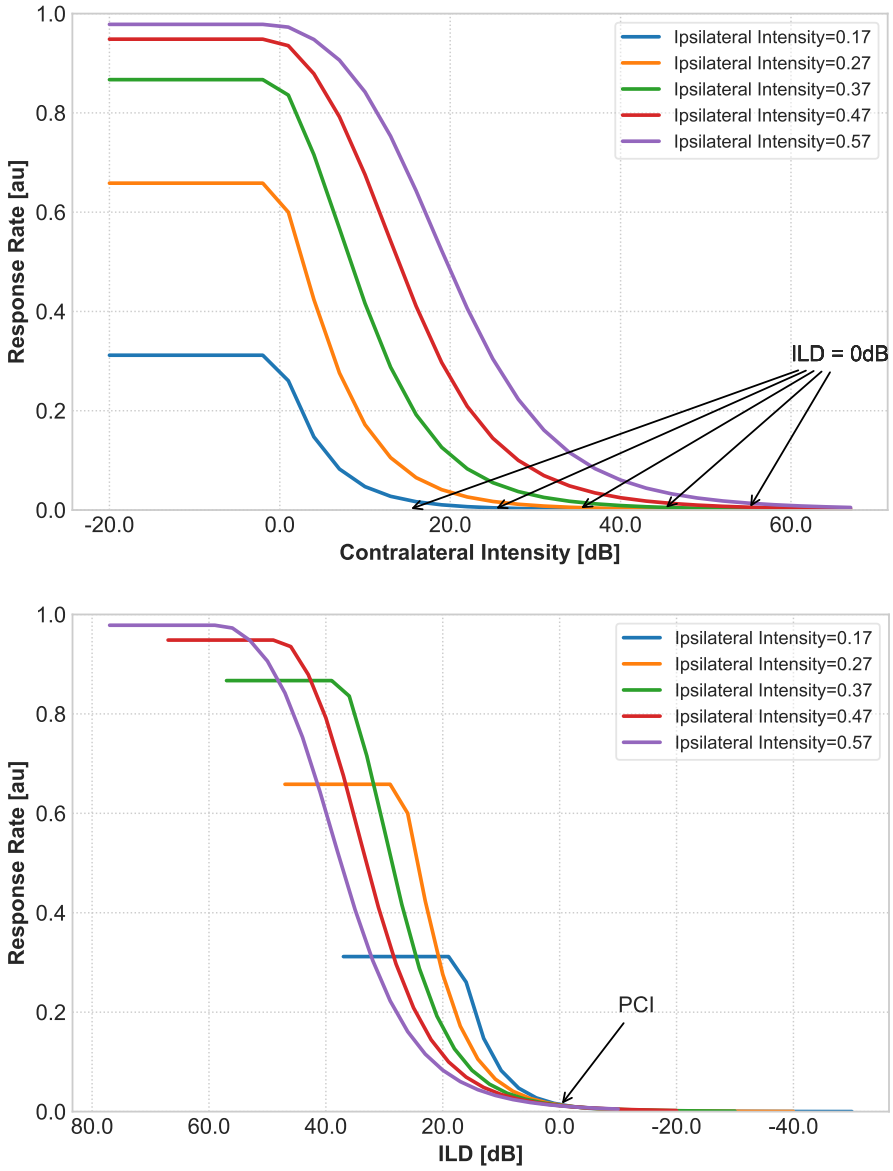

Fig 20. Upper plot displays the neuron response for different ipsilateral input intensities over contralateral input intensities as in [21] their Fig. 3. Lower plot summarizes the results in the standard ILD plot. Different colors indicate various ipsilateral input intensities.